AD/A-005 402

SIGHT LINE AUTOPILOT: A NEW CONCEPT IN AIR WEAPONS

Bradford W. Parkinson, et al

Air Force Academy, Colorado

March 1973

062141

SIGHT LINE AUTOPILOT: A NEW CONCEPT IN AIR WEAPONS

by

LT COL B. W. PARKINSON
CAPTAIN M. W. WYNNE
CAPTAIN L. R. KRUCZYNSKI

RESEARCH REPORT 73-4
MARCH 1973

UNITED STATES AIR FORCE ACADEMY
COLORADO 80840

Unclassified
Security Classification

DOCUMENT CONTROL DATA - R & D AD/A-005402

(Security classification of title, body of abstract and indexing annotation must be entered when the overall report is classified)

1. ORIGINATING ACTIVITY (Corporate author)

Hq USAFA (Directorate of Faculty Research)
USAF Academy, Colorado 80840

2a. REPORT SECURITY CLASSIFICATION

Unclassified

2b. GROUP

3. REPORT TITLE

AC-130 Gunship Research Report
Sight Line Autopilot

4. DESCRIPTIVE NOTES (Type of report and inclusive dates)

Research Report

5. AUTHOR(S) (First name, middle initial, last name)

Lt Col Bradford W. Parkinson
Capt Michael W. Wynne
Capt Leonard R. Kruczynski

6. REPORT DATE	7a. TOTAL NO. OF PAGES	7b. NO. OF REFS
March 1973	38	3

8a. CONTRACT OR GRANT NO	9a. ORIGINATOR'S REPORT NUMBER(S)
b. PROJECT NO.	
c.	9b. OTHER REPORT NO(S) (Any other numbers that may be assigned this report)
d.	

10. DISTRIBUTION STATEMENT

Distribution of this document is unlimited.

11. SUPPLEMENTARY NOTES	12. SPONSORING MILITARY ACTIVITY
	Dept of Astronautics and Computer Science USAF Academy, Colorado 80840

13. ABSTRACT

Although the accuracy of the sidefiring AC-130 aircraft is excellent relative to other weapon systems, a detailed error analysis reveals that the pilot is by far the primary source of remaining error. This report concludes that the accuracy of his pointing the aircraft could be dramatically improved if the sight line were aimed automatically. The sight line autopilot (SLAP) is designed to meet this need. The autopilot design accounts for the linearized motions of the sight line as seen in the pilot's reference frame and adjoins these to the aircraft attitude states and two oscillating wind states.

Using optimal regulator theory, the aircraft control gains are generated. Using these gains, extensive computer simulations were run to check the autopilot's control. Included were winds and sensor noise. The results show that the concept of a SLAP will significantly improve the capability of the widefiring weapons system and allow the pilot to concentrate on aiming the weapons.

DD FORM 1 NOV 65 1473

Unclassified
Security Classification

14. KEY WORDS	LINK A		LINK B		LINK C	
	ROLE	WT	ROLE	WT	ROLE	WT
Optimal Control						
Weapons Systems						
Fire Control						
AC-130 Gunship						
Sightline Autopilot						
Sidefiring						
Linear Regulator						
Linear Quadratic Loss Program						

SIGHT LINE AUTOPILOT:
A NEW CONCEPT IN AIR WEAPONS

by

Lt. Col. B. W. Parkinson
Captain M. W. Wynne
Captain L. R. Kruczynski

UNITED STATES AIR FORCE ACADEMY

RESEARCH REPORT 73-4

MARCH 1973

Editorial Review by Captain J. B. McTasney
Department of English

This Research Report is presented as a competent treatment of the subject, worthy of publication. The United States Air Force Academy vouches for the quality of the research, without necessarily endorsing the opinions and conclusions of the authors.

TABLE OF CONTENTS

LIST OF FIGURES

Abstract

Although the accuracy of the sidefiring AC-130 aircraft is excellent relative to other weapon systems, a detailed error analysis reveals that the pilot is by far the primary source of remaining error. This report concludes that the accuracy of his pointing the aircraft could be dramatically improved if the sight line were aimed automatically. The sight line autopilot (SLAP) is designed to meet this need. The autopilot design accounts for the linearized motions of the sight line as seen in the pilot's reference frame and adjoins these to the aircraft attitude states and two oscillating wind states.

Using optimal regulator theory, the aircraft control gains are generated. Using these gains, extensive computer simulations were run to check the autopilot's control. Included were winds and sensor noise. The results show that the concept of a SLAP will significantly improve the capability of the sidefiring weapons system and allow the pilot to concentrate on aiming the weapons.

INTRODUCTION

The development of the gunship concept for air warfare has progressed steadily since the early operation of the AC-47 "Dragonships" through the initiation of the AC-130 model aircraft into the program. The degree of sophistication has also increased from an area coverage device, which required little accuracy, to a designated target device, requiring a high degree of accuracy. This accuracy requirement demanded a further investigation of error sources in the weapon system.

The U.S. Air Force Academy, as part of the program of research and consulting, has been steadily supplying assistance to the Gunship Office and was requested to conduct the principal investigation of error sources and their possible correction. Early research determined that the pilot was a major error source. This, however, was not entirely his fault. The AC-130 has several slightly damped dutch-roll characteristics which make it very difficult to hold aircraft attitudes to within fractions of a degree. Vastly complicating the picture is the fact that the attack attitude is a steady turn with the guns pointed out the side of the aircraft. Thus, lateral and longitudinal motions are not separable. Furthermore, the required attack mode is to fly at nearly constant altitude and air speed on any given firing run.

The requirements to maintain the necessary flight condition to achieve the accuracy are so severe that the pilot would apparently benefit from a specialized autopilot. This autopilot could hold the weapons on target, even in the face of winds, using a target line. The important thing is to be able to fire and hit the target -- not to fly a circular pattern. Thus, with this autopilot, the target should always lie along the target line which is only slightly affected by fire control corrections or offsets from a constant direction. A problem overview can be obtained from Figure 1. It can be seen that this is a classic regulator problem. The principle complication is that this is at least a twelve state, three input system. Because of the turning condition, it is not easy to separate the modes. Furthermore, because of the interest in maintaining a constant target line, the wind is a very significant factor.

Using linearized dynamics, it is possible to cast this problem in an optimal regulator format that uses a Riccati equation to establish state feedback gains. The optimal design has been verified by extensive simulations including the effect of sensor noise, outside unknown constant error sources, and limiters on the control surface motion. The digital program principally used in this investigation is the Linear Quadratic Loss program created at the University of Florida, by, among others, Captain Charles Fosha (Department of Astronautics and Computer Science, USAFA) as an evolution of previous ASP and

GASP. Extensive modification to the program, notably the technique of spectral factorization to solve the matrix Riccati equation, was accomplished by Captain Fosha in support of the autopilot design. As is true of all numerical programs; certain ruses, described later in this paper, were employed to avoid numerical difficulties.

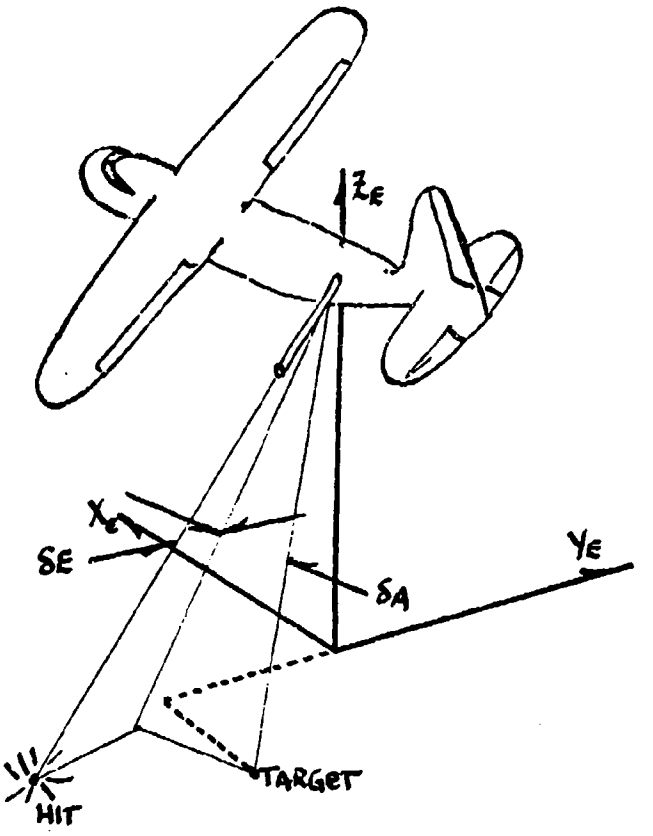

δ_E = Elevation Angle between Sight Line and Target Line

δ_A = Azimuth Angle between Sight Line and Target Line

X_e-Y_e plane is EARTH

Figure 1 - Problem Geometry

DYNAMIC MODEL EQUATIONS

The dynamic model equations for the gunship problem can be derived in two parts. These two parts correspond to (1) the motion of the aircraft with respect to a given air mass, and (2) the motion of a point on the ground with respect to an observer on the aircraft. The development of the linearized equations of motion for an aircraft about a nominal flight condition are well known and shall not be repeated here. For a complete derivation see Dynamics of Flight by Bernard Etkin (Ref).

The linearized states which are used are:

$x_1 = \delta\alpha$ (perturbation to angle-of-attack-radians)

$x_2 = \delta q$ (perturbation to pitch rate-rad/sec)

$x_3 = \delta\beta$ (perturbation to sideslip-radians)

$x_4 = \delta p$ (perturbation to roll rate-rad/sec)

$x_5 = \delta r$ (perturbation to yaw rate-rad/sec)

$x_6 = \delta\phi$ (perturbation to roll angle-radians)

$x_7 = \delta\theta$ (perturbation to pitch angle-radians)

The perturbations are defined as

$$\delta\alpha = \alpha - \alpha_o$$

where α is actual angle-of-attack and α_o is the nominal angle of attack. Similar definitions hold for the perturbations to the remaining states. Since the nominal flight condition is a level equilibrium turn, the nominal values used are constant.

The aircraft equations were used as follows, assuming that nominals sideslip (β_o) is zero.

$$\dot{mu} = (\rho u_o S C_x + 1/2\rho u_o S C_{x_u} - mq_o\alpha_o)u + (1/2\rho u_o^2 S C_{x_\alpha} - mq_o u_o)\alpha$$
$$+(1/4\rho u_o S\bar{c} C_{x_q} - m\alpha_o u_o)q - (mg\cos\theta_o)\theta + (mr_o u_o)\beta$$
$$-(\rho u_o S C_x + 1/2\rho u_o S C_{x_u})u_g - 1/2\rho u_o^2 S(C_{x_\alpha} + \frac{\pi c}{8u_o b} C_{x_q})\alpha g$$
$$-(1/4\rho u_o S\bar{c} C_{x_q})q'g$$

$$m\alpha_o\dot{u} + (mu_o - 1/4\rho u_o S\bar{c} C_{z_{\dot\alpha}})\dot{\alpha} = (\rho u_o S C_z + 1/2\rho u_o S C_z + mq_o)u$$
$$+(1/2\rho u_o^2 S C_{z\alpha})\alpha + (1/4\rho u_o S\bar{c} C_{z_q} + mu_o)q - (mg\cos\phi_o \sin\theta_o)\theta$$
$$-(mu_o p_o)\beta - (mg\sin\phi_o\cos\theta_o)\phi + (1/2\rho u_o^2 S C_{z_{\delta_e}})\delta_e$$
$$-(\rho u_o S C_z + 1/2\rho u_o S C_{z_u})u_g - 1/2\rho u_o^2 S(C_{z_\alpha} + \frac{\pi\bar{c}}{8u_o b} C_{z_q})\alpha g$$
$$-1/4\rho u_o S\bar{c} C_{zq})q'g$$

$$-(1/4\rho u_o S\bar{c}^2 C_{m_{\dot\alpha}})\dot{\alpha} + I_{yy}\dot{q} = (\rho u_o S\bar{c} C_m + 1/2\rho u_o S\bar{c} C_{m_u})u$$
$$-\left[(1/2\rho u_o^2 S\bar{c} C_{m_\alpha})\alpha + (1/4\rho u_o S\bar{c}^2 C_{mq})q + \left[(I_{zz} - I_{xx})r_o - 2I_{xz}p_o\right]p\right.$$
$$\left. + (I_{zz} - I_{xx})p_o + 2I_{xz}r_o\right]r + (1/2\rho u_o^2 S\bar{c} C_{m_{\delta_e}})\delta_e$$
$$-(\rho u_o S\bar{c} C_m + 1/2\rho u_o S\bar{c} C_{m_u})u_g - 1/2\rho u_o^2 S\bar{c}(C_{m_\alpha} + \frac{\pi\bar{c}}{8u_o b} C_{mq})\alpha g$$
$$-(1/4\rho u_o S\bar{c}^2 C_{mq})q'g$$

$$\dot{\theta} = (\cos\phi_o)q - (\sin\phi_o)r - (q_o\sin\phi_o + r_o\cos\phi_o)\phi$$

$$I_{xx}\dot{p} - I_{xz}\dot{r} = (\rho S u_o b C_\ell)u + \left[(I_{yy} - I_{zz})r_o + I_{xz}p_o\right] q$$
$$+(1/4\rho u_o S b^2 C_{\ell p} + I_{xz}q_o)p + \left[1/4\rho u_o S b^2 C_{\ell\ r} - (I_{zz}-I_{yy})q_o\right] r$$
$$+(1/2\rho u_o{}^2 S b C_{\ell_\beta})\beta + (1/2\rho u_o{}^2 S b C_{\ell_{\delta_r}})\delta r + (1/2\rho u_o{}^2 S b C_{\ell_{\delta_a}})\delta a$$

$$-(\rho S u_o b C_\ell)u_g - (1/4\rho u_o S b^2 C_{\ell p})p_g - (1/4\rho u_o{}^2 S b^2 C_{\ell r})r'_g$$
$$-1/2\rho u_o{}^2 S b (C_{\ell\beta} - \frac{\pi}{6u_o} C_{\ell r})\beta_g$$

$$-I_{xz}\dot{p} + I_{zz}\dot{r} = (\rho S u_o b C_n)u + \left[(I_{xx} - I_{yy})p_o - I_{xz}r_o\right] q$$
$$+ \left[1/4\rho u_o S b^2 C_{n_p} - (I_{yy} - I_{xx})\ q_o\right] p + (1/4\rho u_o S b^2 C_{n_r} - I_{xz}q_o)r$$
$$-(1/2\rho u_o{}^2 S b C_{n\beta})\beta + (1/2\rho u_o{}^2 S b C_{n_{\delta_r}})\delta r + (1/2\rho u_o{}^2 S b C_{n_{\delta_a}})\delta a$$
$$-(\rho S u_o b C_n)u_g - (1/4\rho u_o S b^2 C_{n_p})p_g - (1/4\rho u_o{}^2 S b^2 C_{n_r})r'_g$$
$$-1/2\rho u_o{}^2 S b (C_{n\beta} - \frac{\pi}{6u_o} C_{n_r})\beta_g$$

$$m u_o \dot{\beta} = (\rho u_o S C_y - m r_o + m p_o \alpha_o)u + (m p_o u_o)\alpha - (mg \sin\phi_o \sin\theta_o)\theta$$
$$+(1/4\rho u_o S b C_{y_p} + m\alpha_o u_o)p + (1/4\rho u_o S b C_{y_r} - m u_o)r$$
$$+(1/2\rho u_o{}^2 S C_{y_\beta})\beta + (mg \cos\phi_o \cos\theta_o)\phi + (1/2\rho u_o{}^2 S C_{y_{\delta_r}} - (\rho u_o S C_y)u_g$$
$$-(1/4\rho u_o S b C_{y_p})p_g - (1/4\rho u_o S b C_{yr})r'_g - 1/2\rho u_o{}^2 S (C_{y_\beta} - \frac{\pi}{6u_o} C_{y_r})\beta_g$$

$$\dot{\phi} = (\sin\phi_o \tan\theta_o)q + \left[(q_o \sin\phi_o + r_o \cos\phi_o)\sec^2\theta_o\right]\theta + p$$
$$+(\cos\phi_o \tan\theta_o)r + \left[(q_o \cos\phi_o - r_o \sin\phi_o)\tan\theta_o\right]\phi$$

The aircraft states which are not used are azimuth (ψ), (which is cyclic) and velocity variation (δu) which is maintained at zero by the copilot or a separate control device.*

POSITION DYNAMIC EQUATIONS

The gunship, during its attack maneuver, attempts to maintain the target in a very nearly fixed position in the aircraft coordinate frame. This position is on the left beam and below the wing line. Thus, the aircraft flies a modified pylon turn about the target. For this reason it is natural to select an aircraft oriented coordinate frame in order to define the translational position of the aircraft. In other words, the autopilot will attempt to position the target out the left wing and down, using the coordinates Range (R), Elevation (E), and Azimuth (A) which are defined in Figure 2.** A second independent set of translational coordinates is altitude (H), with E and A as previously defined. The change of reference frames from range to altitude is a simple transformation and is accomplished later in this section. The three additional states are designated as follows:

x_8 = R (range-feet)
x_9 = E (elevation angle of sight line-radians)
x_{10} = A (azimuth angle of sight line-radians)

A forcing function due to wind will be included in the derivation.

---

*This state will probably be added to the problem along with a throttle control variable at a later time.

**Note the nominal elevation angle is negative, nominal azimuth is zero and nominal range is the slant range to the target.

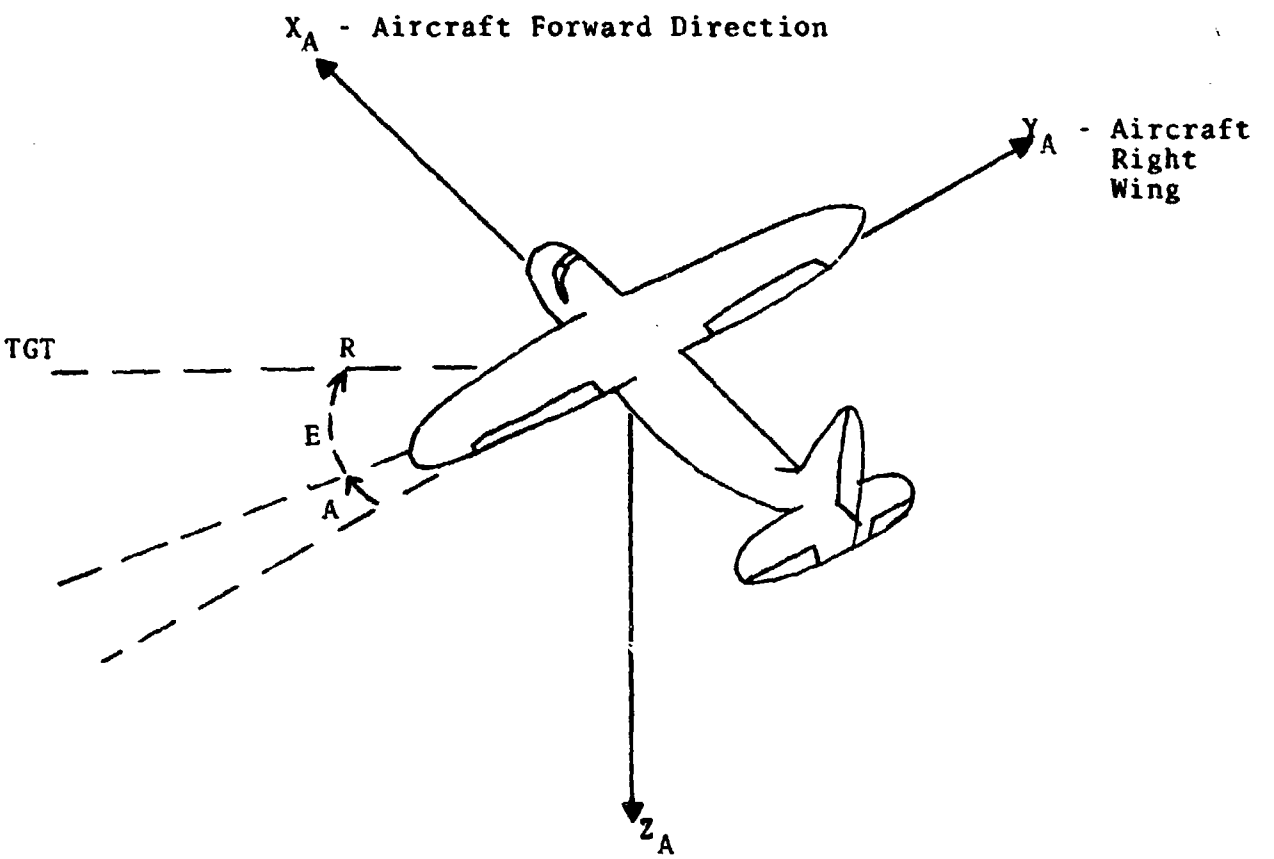

Figure 2 - Definition of Target Position Coordinates

The time derivative of the radius vector in the earth frame consists of the velocity of the aircraft in the air mass and the motion of the air mass. Expressed in the aircraft oriented frame, the velocity of the aircraft with respect to a point in the air mass is

$$\begin{bmatrix} u \cos \alpha \cos \beta \\ u \cos \alpha \sin \beta \\ u \sin \alpha \cos \beta \end{bmatrix}$$

where u is the total velocity of the aircraft in feet per second.

If the target is considered a stationary point on the ground and the winds are constant, the velocity of the air mass with respect to the target is

$$\begin{bmatrix} -V_W \cos \psi \\ V_W \sin \psi \\ -V_V \end{bmatrix}$$

where V_W is the horizontal wind component, V_V is the vertical wind component and ψ is the angle in the horizontal plane from the wind direction to the projection of the aircraft x-direction (nose).* So, the velocity of the aircraft with respect to the target and the velocity of the air-

*ψ = aircraft heading - wind direction = $\psi_a - \psi_W$

craft with respect to the air mass can be expressed as:

$$\begin{bmatrix} u\cos\alpha\cos\beta \\ u\cos\alpha\sin\beta \\ u\sin\alpha\cos\beta \end{bmatrix} + \begin{bmatrix} 1 & 0 & 0 \\ 0 & \cos\phi & \sin\phi \\ 0 & -\sin\phi & \cos\phi \end{bmatrix} \begin{bmatrix} \cos\theta & 0 & -\sin\theta \\ 0 & 1 & 0 \\ \sin\theta & 0 & \cos\theta \end{bmatrix} \begin{bmatrix} -V_W\cos\psi \\ -V_W\sin\psi \\ -V_V \end{bmatrix}$$

The θ and ϕ transformations are required to take the wind velocity from the horizontal plane to the aircraft (x,y) plane as illustrated in Figure 3. Since this represents the velocity of the aircraft with respect to the target as measured in the earth's frame, the velocity of the target with respect to the aircraft requires only a sign change. The result is

$$\overset{E}{\underset{R}{\overset{*}{}}}_{A} = \begin{bmatrix} -u\cos\alpha\cos\beta \\ -u\cos\alpha\sin\beta \\ -u\sin\alpha\cos\beta \end{bmatrix} + \begin{bmatrix} 1 & 0 & 0 \\ 0 & \cos\phi & \sin\phi \\ 0 & -\sin\phi & \cos\phi \end{bmatrix}$$

$$\begin{bmatrix} \cos\theta & 0 & -\sin\theta \\ 0 & 1 & 0 \\ \sin\theta & 0 & \cos\theta \end{bmatrix} \begin{bmatrix} V_W\cos\psi \\ -V_W\sin\psi \\ V_V \end{bmatrix}$$

where $\underset{A}{R}$ is the radius vector from the aircraft to the target as shown in Figure 2.

The "Coriolis Law" is now used to find the relationship between $\overset{E}{\underset{R}{}}_{A}$ and the time derivative of $\underset{A}{R}$ in the aircraft

$\overset{*}{(\ )}$
$\underset{[\ ]}{X}$ - Vector X; expressed in [ ] corrdinates, with time derivative in ( ) coordinates.

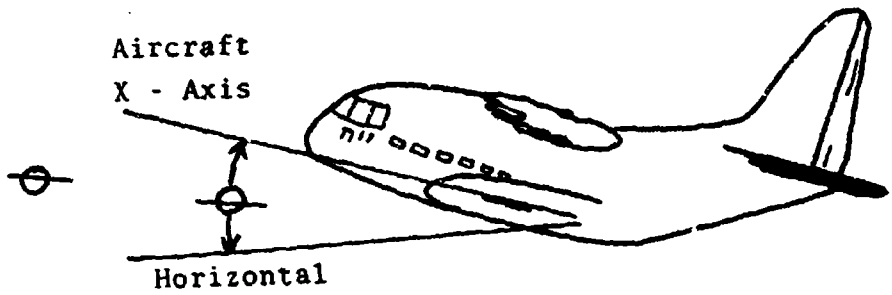

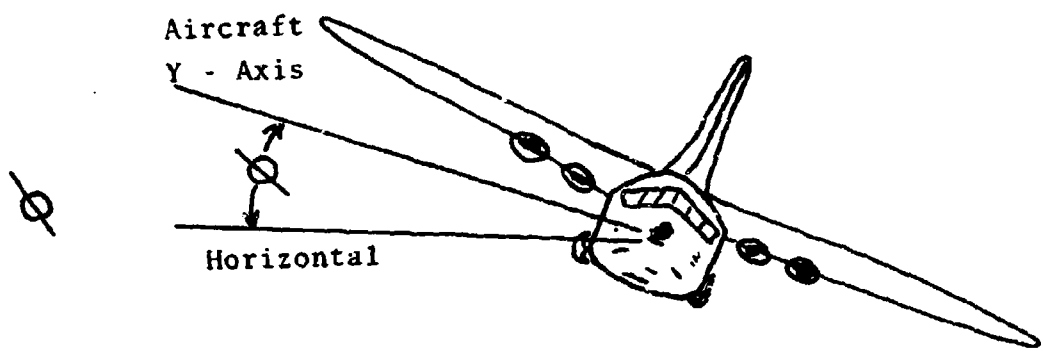

FIGURE 3 Pitch Angle

Bank Angle

Definitions

frame $\begin{pmatrix} A \\ R \\ A \end{pmatrix}$.

$$\begin{matrix} E \\ R \\ A \end{matrix} = \begin{matrix} A \\ R \\ A \end{matrix} + \underline{\omega}_{A/E} \times \begin{matrix} R \\ A \end{matrix} \tag{2}$$

$\underline{\omega}_{A/E}$ is the angular rate of the aircraft with respect to the earth.

Referring to Figure 2, $\begin{matrix} R \\ A \end{matrix}$ can be represented as

$$\begin{matrix} R \\ A \end{matrix} = \begin{bmatrix} R \cos E \sin A \\ -R \cos E \cos A \\ -R \sin E \end{bmatrix} \tag{3}$$

The aircraft angular rate vector

$$\underline{\omega}_{A/E} = \begin{bmatrix} p \\ q \\ r \end{bmatrix}$$

can be expressed as the matrix

$$\begin{bmatrix} 0 & -r & q \\ r & 0 & -p \\ -q & p & 0 \end{bmatrix} = (\underline{\omega}_{A/E}{}^{x}) \tag{4}$$

to evaluate the cross product term in matrix muliplication form; i.e.,

$\underline{\omega}_{A/E} \times \frac{R}{A}$ is replaced with

$$\begin{bmatrix} 0 & -r & q \\ r & 0 & -p \\ -q & p & 0 \end{bmatrix} \begin{bmatrix} R \cos E \sin A \\ -R \cos E \cos A \\ -R \sin E \end{bmatrix} \qquad (5)$$

Now, to fill in for $\frac{A}{R}_{\overline{A}}$, the time derivative of Equation (3) as run in the ^{A} aircraft frame is taken

$$\frac{A}{R}_{\overline{A}} = \begin{bmatrix} \dot{R} \cos E \sin A - R \sin E \sin A\dot{E} + R \cos E \cos A\dot{A} \\ -\dot{R} \cos E \cos A + R \sin E \cos A\dot{E} + R \cos E \sin A\dot{A} \\ -\dot{R} \sin E - R \cos E\dot{E} \end{bmatrix}$$

Equation (2) is now represented as

$$\begin{bmatrix} -u \cos\alpha \cos\beta \\ -u \cos\alpha \sin\beta \\ -u \sin\alpha \cos\beta \end{bmatrix} + \begin{bmatrix} 1 & 0 & 0 \\ 0 & \cos\phi & \sin\phi \\ 0 & -\sin\phi & \cos\phi \end{bmatrix} \begin{bmatrix} \cos\theta & 0 & -\sin\theta \\ 0 & 1 & 0 \\ \sin\theta & & \cos\theta \end{bmatrix} \begin{bmatrix} V_W \cos\psi \\ -V_W \sin\psi \\ V \end{bmatrix} =$$

$$\begin{bmatrix} \dot{R} \cos E \sin A - R \sin E \sin A\dot{E} + R \cos E \cos A\dot{A} \\ -\dot{R} \cos E \cos A + R \sin E \cos A\dot{E} + R \cos E \sin A\dot{A} \\ -\dot{R} \sin E - R \cos E\dot{E} \end{bmatrix} \qquad (6)$$

$$+\begin{bmatrix} 0 & -r & q \\ r & 0 & -p \\ -q & p & 0 \end{bmatrix} \begin{bmatrix} R\cos E \sin A \\ -R\cos E \cos A \\ -R \sin E \end{bmatrix} \qquad (6)$$

Equation (6) can be solved for the line-of-sight states

$$\begin{bmatrix} \dot{\delta R} \\ \dot{\delta E} \\ \dot{\delta A} \end{bmatrix} = \begin{bmatrix} \dot{x}_8 \\ \dot{x}_9 \\ \dot{x}_{10} \end{bmatrix}$$

and linearized about given nominal conditions. Assumptions regarding the nominal condition are:

1) small angle approximations used for α_o, θ_o, δE, δA

2) $\beta_0 = 0$, $A_o = 0$

The result is shown in Equation (8).

$$\begin{bmatrix} \dot{\delta R} \\ \dot{\delta E} \\ \dot{\delta A} \end{bmatrix} = \begin{bmatrix} u_o sE_o & 0 & u_o cE_o & 0 & 0 & 0 & 0 & 0 \\ u_o cE_o/R_o & 0 & -u_o sE_o/R_o & -1 & 0 & 0 & 0 & -p_o/R_u \\ 0 & \tan E_o & 0 & 0 & -1 & 0 & 0 & (q_o \tan E_u - r_o)/R_o \end{bmatrix}$$

$$\begin{bmatrix} p_o R_o & R_o cE_o(r_o cE_o - q_o sE_o) & -\theta_o s(\phi_o + E_o) & c(\phi_o + E_o) \\ 0 & -cE_o(r_o sE_o + q_o cE_o) & -\theta_o c(\phi_o + E_o)/R_o & 0 \\ r_o \tan E_o + q_o & 0 & 1/R_o cE_o & -s(\phi_o + E_o)/R_o \end{bmatrix} X \qquad (8)$$

THE WIND DYNAMICAL EQUATIONS

From the seven air mass states and the three line-of-sight states, we define two states which consider the wind effects:

$$x_{11} = V_W \cos \psi \quad \text{(wind along the A/C heading)}$$

$$x_{12} = V_W \sin \psi \quad \text{(cross wind)}$$

Taking the derivatives of the wind states and linearizing

$$\dot{x}_{11} = V_W \sin \psi\dot{\psi} = -x_{12}\dot{\psi} \simeq -x_{12}\dot{\psi}_o$$

$$\dot{x}_{12} = V_W \cos \psi\dot{\psi} = x_{11}\dot{\psi} \simeq x_{11}\dot{\psi}_o$$

CONVERSION TO H, A, E

There is a second set of position states which is possibly more useful, depending upon the availability of sensors, since we are ultimately concerned with state feedback. This second set uses altitude H, and the two angles E and A. To derive the second set, two relations, one static and one dynamic, are established for altitude.

The static relation is obtained by transforming the $\frac{R}{A}$ vector through the angles θ and ϕ to the earth frame

$$\begin{bmatrix} \cos\theta & \sin\phi\sin\theta & \cos\phi\sin\theta \\ 0 & \cos\phi & -\sin\phi \\ -\sin\theta & \sin\phi\cos\theta & \cos\phi\cos\theta \end{bmatrix} \begin{bmatrix} R\cos E\sin A \\ -R\cos E\cos A \\ -R\sin E \end{bmatrix}$$

Altitude is found in the third component:

$$-R \cos E \sin A \sin \theta - R \cos E \cos A \sin \phi \cos \theta - R \sin E \cos \phi \cos \theta$$

Using small angle approximations for θ and A and a trigonometric identity for $\sin(\phi+E)$, we obtain

$$H = -R \sin(\phi+E) - R\theta A \cos E$$

The dynamic relationship is similarly obtained by transforming the aircraft velocity in the air mass through the angles ϕ and θ and determining the third component. The result is:

$$\dot{H} = u \cos \alpha \cos \beta \sin \theta - u \cos \alpha \sin \beta \sin \phi \cos \theta - u \sin \alpha \cos \beta \cos \phi \cos \theta$$

Using the small angle approximations for α, β and ϕ, results in

$$\dot{H} = u\theta - u\beta \sin \phi - u\alpha \cos \phi$$

Equation (8) can now be replaced with Equation (9), which is on the following page.

The seven aircraft states, the three position states, and the two wind states form the dynamic plant for the

$$\begin{bmatrix} \delta\dot{H} \\ \delta\dot{E} \\ \delta\dot{A} \end{bmatrix} = \begin{bmatrix} -u_o c\phi_o & 0 & -u_o s\phi_o & 0 & 0 & u_o(\alpha_o s\phi_o - \beta_o c\phi_o) & u_o \\ u_o cE_o/R_o & 0 & -u_o sE_o/R_o & -1 & 0 & p_o c(E_o+\phi_o)/s(\phi_o+E_o) & 0 \\ 0 & \tan E_o & 0 & 0 & -1 & (r_o - q_o \tan E_o)c(E_o+\phi_o)/s(E_o+\phi_o) & 0 \end{bmatrix}$$

$$\begin{matrix} 0 & \cdots & 0 & 0 \\ \dfrac{p_o}{R_o s(E_o+\phi_o)} & & p_o c(E_o+\phi_o)/s(E_o+\phi_o) & -cE_o(r_o E_o + q_o cE_o) + \dfrac{\theta_o p_o cE_o}{s(E_o+\phi_o)} \end{matrix} \qquad (9)$$

16a

$$\begin{matrix} (r_o - Q_o \tan E_o)/R_o s(E_o+\phi_o) & (r_o \tan E_o + q_o) + \dfrac{(r_o - Q_o \tan E_o)}{s(E_o+\phi_o)} c(E_o+\phi_o) & \dfrac{-\theta_o}{s(E_o+\phi_o)}(q_o sE_o - r_o cE_o) \end{matrix}$$

$$\begin{bmatrix} 0 & 0 \\ -\dfrac{\theta_o}{R_o} c(\phi_o+E_o) & \dfrac{-s(\phi_o+E_o)}{R_o} \\ 1/R_o cE_o & 0 \end{bmatrix} \bar{X}$$

problem. The control elements chosen are the aircraft control surfaces. That is:

$u_1 = \delta R_u$; Rudder

$u_2 = \delta A_e$; Aileron

$u_3 = \delta E_L$; Elevator

Conspicuously left out here is a throttle control; however, recall that for other reasons, the throttle or (δ_u) is maintained at zero.

The system we have defined here is of twelve coupled states with three independent inputs. This forms a linear dynamic plant. The next section details the problem formulation in the classic linear optimization method, and explains some details of the optimization method.

FEEDBACK CONTROL SYNTHESIS

The problem being addressed is that of a linear regulator. The solution for quadratic penalties, using optimal control theory is explained in reference 2, Bryson and Ho. The results will be briefly reviewed here to establish notation. Given the system

$$\dot{\underline{x}} = F\underline{x} + G\underline{u}$$

with $\underline{x}$ and nxl state vector

$\underline{u}$ an mxl control vector

F an nxn system matrix

G an nxm control distribution matrix

minimize the Performance Index (J)

$$J = \tfrac{1}{2}\int_{t_o}^{t_f} (\underline{x}^T A\underline{x} + \underline{u}^T B\underline{u})dt$$

where A is an nxn positive-semidefinite matrix

and B is an mxm positive definite matrix

The steady state solution; i.e., for large t_f, is found by solving the Riccati equation "backwards" in time:

$$\dot{S} = -SF - F^T S + SGB^{-1} G^T S - A \qquad (10)$$

until it reaches a stabilized value of S(a constant).

This S is then used to specify the feedback matrix C:

$$\underline{u} = C\underline{x}$$

$$C = -B^{-1}G^{T}S$$

So the optimum system "closed loop" equation is:

$$\dot{\underline{x}} = [F - GB^{-1}G^{T}S]\underline{x}$$

This theoretical problem is solved at USAFA using the Linear Quadratic Loss program. The solution to the steady state version of (8) is performed algebraically using Potter's method. This depends on solving for the eigenvalues and eigenvectors of a 2n x 2n matrix. Unfortunately, repeated roots give rise to numerical difficulties, as do undamped roots. The following problems were encountered as a result.

a. Regulating to non-zero values. Each state which is called on to regulate to a non-zero value can be handled by adding an additional integrator which has an initial condition equal to the desired offset value, and no input. The state weighting matrix (A) is then expanded to include the additional state, and the quadratic form (A) is adjusted to weight the <u>difference</u> between actual and desired squared.

This led to two numerical problems. There are three off-nominal commands that are useful: those for azimuth (A-state 10), for altitude (H-state 8) and for elevation

(E-state 11). The three integrators represent three repeated zero roots and prevented a numerical solution. This was solved, however, by lightly damping each of the integrators, (i.e., time constants of 10^6 seconds) slightly differently. There was no appreciable change in state during the duration of the problem. However, the eigenvectors could now be found using a double-precision routine on the computer. The second difficulty was that numerical rounding would sometimes cause the weighing matrix A to appear indefinite to the computer. This was solved by allowing the diagonal terms to slightly dominate the off-diagonal ones.

b. The Wind Oscillator. Because the eigenvalues of the wind oscillator (states 11 and 12) are purely imaginary, the Potter method creates a repeated pair. This is because all system eigenvalues and a corresponding set which is reflected about the imaginary axis are present. This problem is solved by adding a very slight amount of damping to the wind oscillator.

c. Hydraulic Servo Lags. To validate the performance of the autopilot design, servo lags estimated to be .1 second were added to each actuator. Digital difficulties due to the repeated roots were quickly resolved by adding a small separation between the three time constants.

The selection of the matrices A and B was initially made on the basis of the Bryson rule (reference 2, page 149). That is, weights on A, E and H which were inversely proportional to the acceptable maxima; and weights on control which are inversely proportional to the maximum desired control deflections. The resulting system tended to respond so quickly that rigid body assumptions were suspect. To solve this, weights were added to the body angular rates until the digital simulation demonstrated reasonable behavior for the assumed range of initial conditions.

RESULTS

In order to verify theoretically the control solution obtained by solving the linear regulator problem, three cases were simulated. The cases presented are in order of increasing difficulty. The cases were simulated for 100 seconds, or approximately two orbits.

Case 1 - Error in Position Given No Wind and No Exterior Disturbance

The first case is presented as a basis for comparison against the more difficult second and third cases. The initial conditions are as follows:

$$\delta h = 100 \text{ ft}; \quad \delta A = \delta E = 3^\circ$$

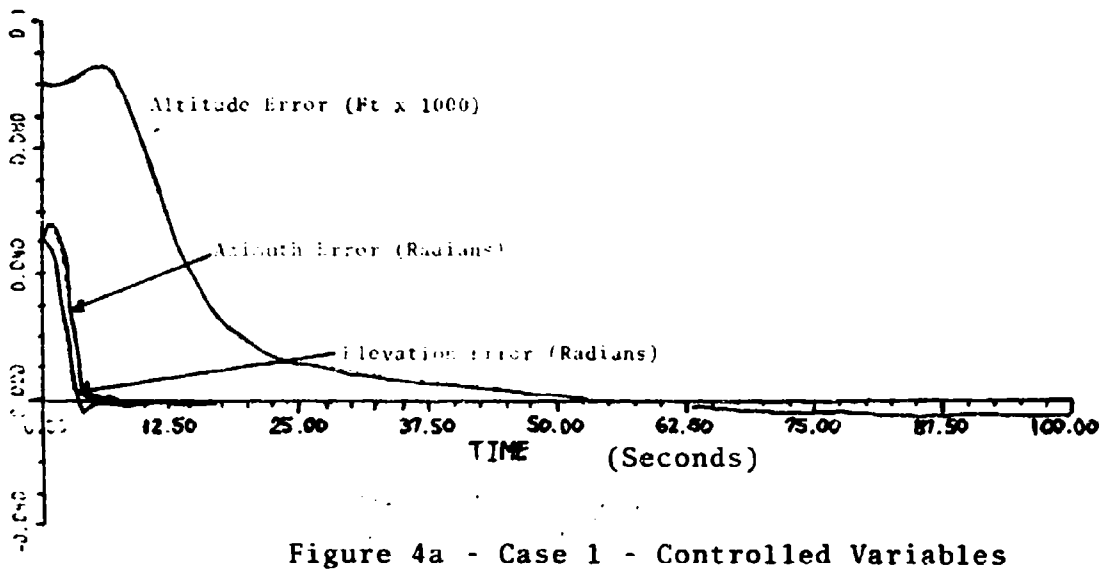

Figure 4a - Case 1 - Controlled Variables

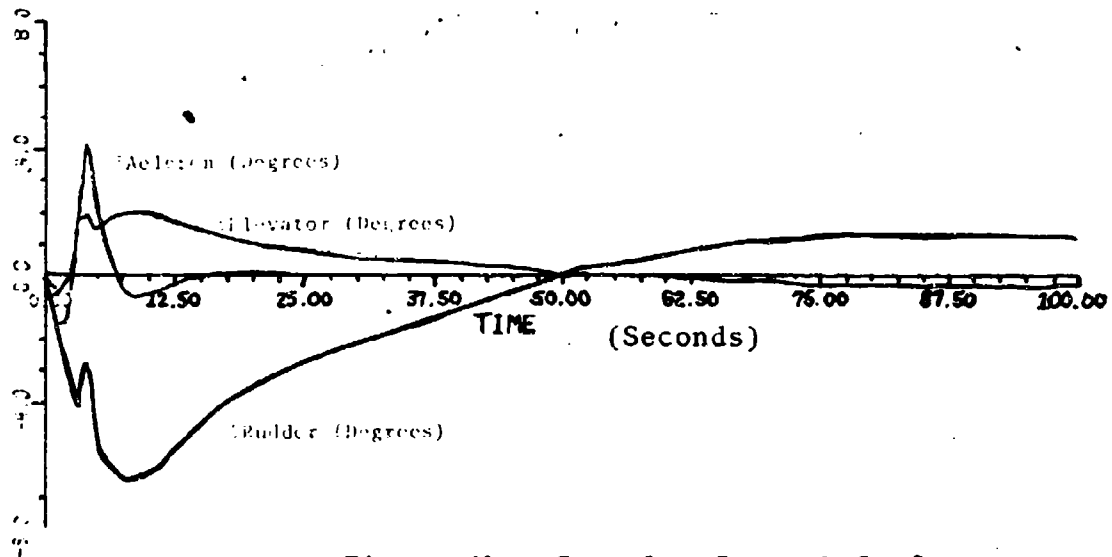

Figure 4b - Case 1 - Control Surfaces

The results in this case are given in Figure 4 (a & b). The influence of weighting the p, q and r attitude states is immediately apparent as the position errors slowly damp towards zero. Without this weighting the practicality of the controller would be negligible due to real control saturation and excessive "g" forces impacting the crew of the aircraft. The control surface deviation is given in the lower graph and is well within practical aircraft limits.

Case 2 - Error in Position Given a Constant Wind But No External Disturbance

Although not shown, it is logical that the path flown will not be wholly circular, but rather an ellipsoid. Case 2 illustrates the capability of the autopilot to maintain a near zero error with wind. The initial conditions are as follows:

wind = 40 ft/sec head on

δh = 100 feet; $\delta A = \delta E = 3°$

Presently, in the constant wind condition, the pilot cannot maintain contact with the target for greater than one-half a turn. The results of the theoretical simulation clearly show (Figure 5 (a & b)) that contact is possible throughout the two-orbit period. The errors are small in

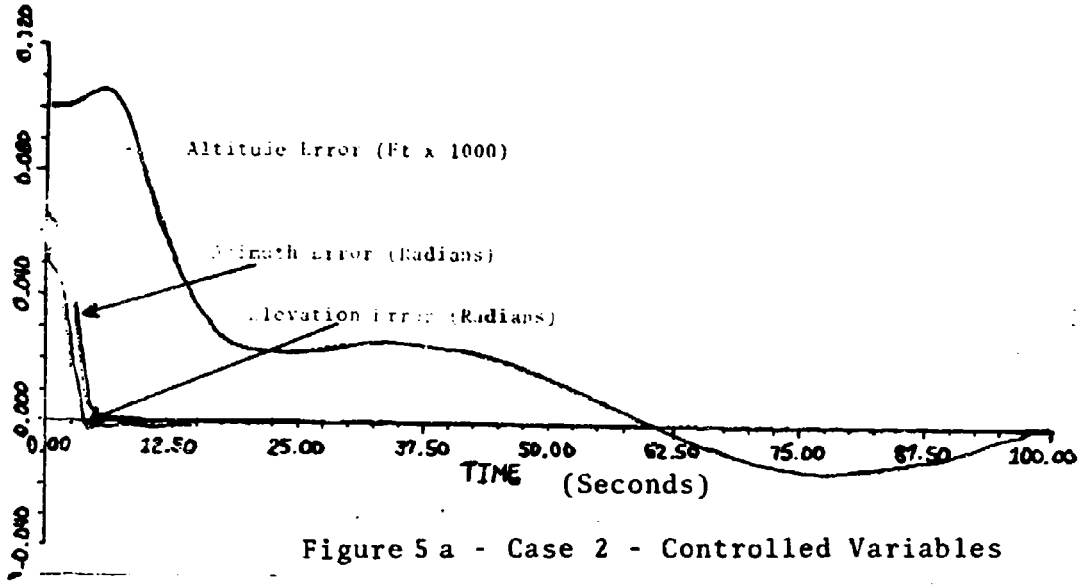

Figure 5 a - Case 2 - Controlled Variables

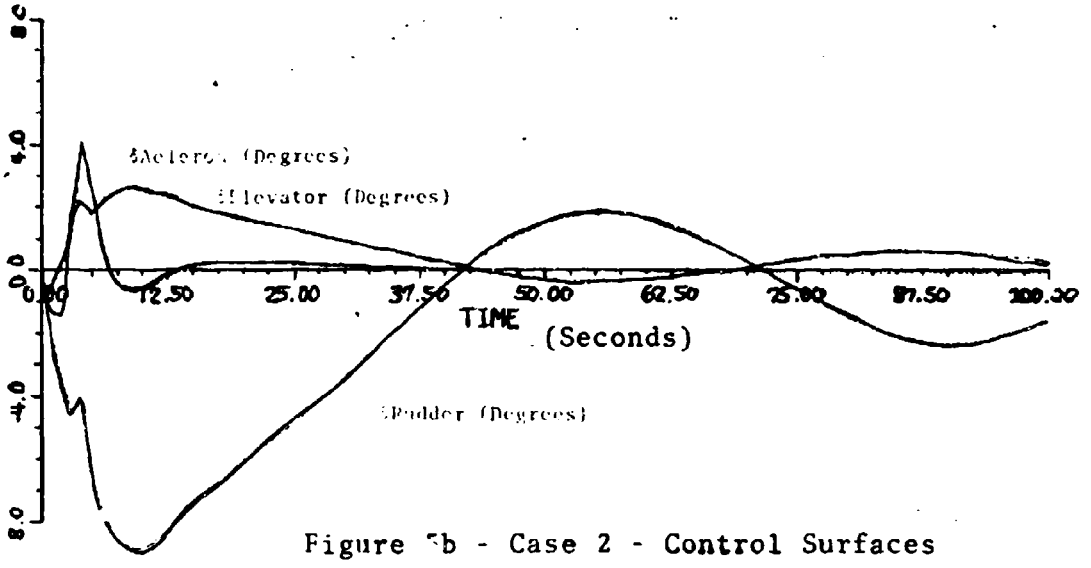

Figure 5b - Case 2 - Control Surfaces

magnitude, though cyclic, and will have only a minor effect on the accuracy of the weapons system. The largest relative error occurs in altitude. This, however, has the least effect on the weapon delivery.

The control surface deviations are still small, however, considerably larger than those in Case 1. It is notable, however, that there are no rapid changes in control surfaces, even at the start and that the largest deviation remains well within the aircraft operating range.

Case 3 - Error in Position Given a Gusting Wind and External Disturbance on All System States

The noise introduced in this case is entered as unknown error sources, assuming that the measurements remain known. The nominal errors used for initial conditions are as follows:

wind = 40 ft/sec head on

δh = 100 ft; $\delta A = \delta E = 3°$

This case is illustrated by Figures 6 (a & b). The path flown by the aircraft is again an ellipsoid, with the added difficulty of the external unknown errors. Once again, the control gains are capable of maintaining target contact throughout the two-orbit period. The accuracy, as expected, is impaired by the external errors; however, the number

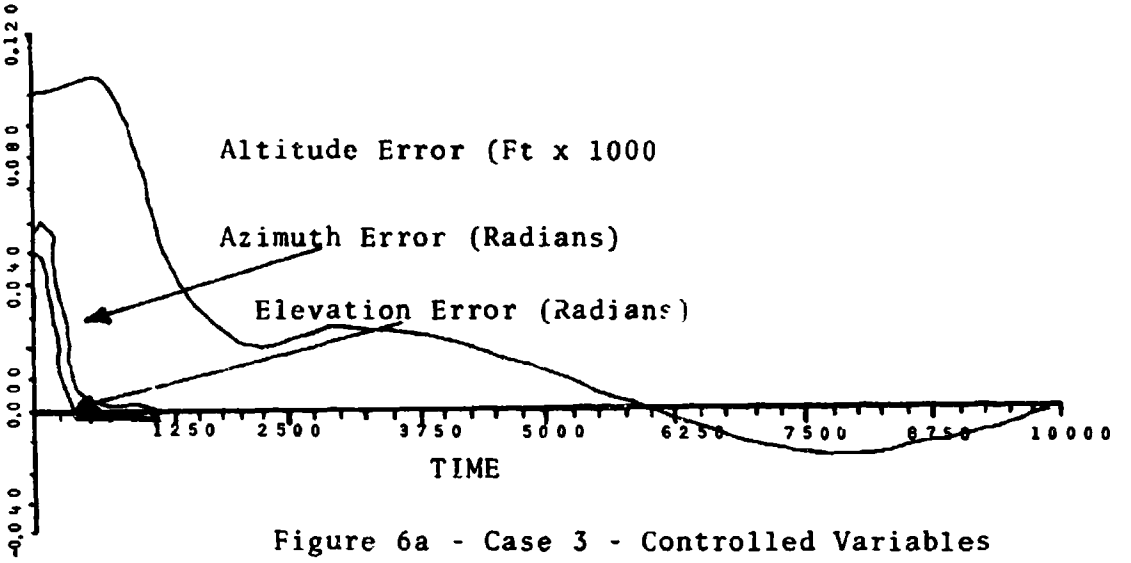

Figure 6a - Case 3 - Controlled Variables

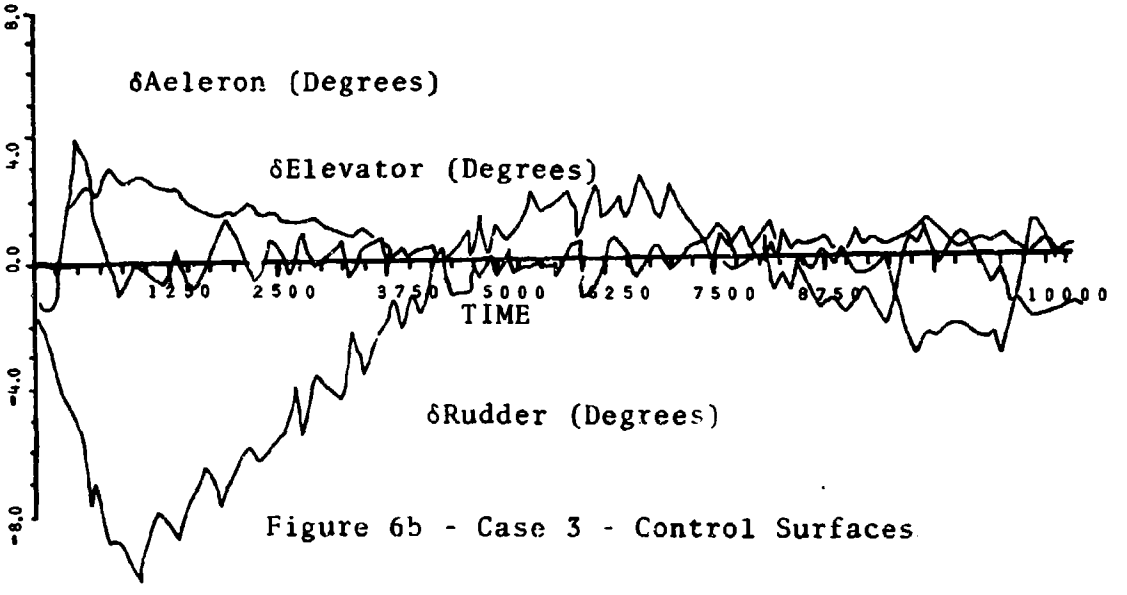

Figure 6b - Case 3 - Control Surfaces

of firing opportunities increases tremendously when contact is maintained. The largest error occurs once again in altitude. For this case the total magnitude of the error is larger than Case 2; however, it is well within its expected value, and should improve much farther with the application of modern filtering techniques.

The control curves (Figure6b) reflect the increased difficulty of the firing problem. Once again the control deviations are within the operating limits, and the changes incurred are incurred smoothly. The servo lags in the control surfaces have filtered to a large extent the higher frequency errors.

HARDWARE

The sight line autopilot is part of a funded Air Force development program. A contract has been let to Minneapolis Honeywell to determine the exact details based on the studies performed at USAFA. It is clear that all state variables should be instrumented. To accommodate different gain values for different flying configurations a digital computer is very desirable, and probably will be part of the test aircraft configurations. The SLAP will probably parallel existing flight hardware and consequently offer a redundant control method in the event of battle damage.

CONCLUSIONS

The complexity of the autopilot design, and the linearization of the dynamic equations about a nominal flight condition made the problem ideal for optimal control theory. With the necessity for observing all states, a Kalman filter becomes a possibility.

The results clearly show that theoretically the addition of the sight line autopilot will greatly enhance the accuracy of the gunship operation. The results do not show the increase in pilot potential due to relieving him of the targeting problem. The resulting controller will be able to theoretically control the side-firing aircraft sight line to an accuracy of better than one mil. This development should significantly advance the capability of weapons systems of this type.

REFERENCES

1. Etkin, Bernard. Dynamics of Flight, John Wiley and Sons, Inc., New York, 1959.

2. Bryson, A. E. and Yu-Chi Ho. Applied Optimal Control, Blaisdale Publishing Company, Waltham, Massachusetts, 1969.

3. "LQL - A General Purpose Program for Control Estimation and Similations," C. E. Fosha, T. E. Bullock, Proceedings of Second Asilomar Conference on Circuits and Systems, Pacific Grove, California, 1968.

4. "Sight Line Auto-Pilot: A new concept in Air Weapons" Lt Col B. W. Parkinson, Capt L. R. Kruezynski, Capt Capt M. W. W. Wynne, AIAA Paper #71-960, August 1971

5. "An Optimal Model-Following Flight Control System for Manual Control", A. J. VanDierendonck, M. Wynne, L. Kryczynski, AIAA Paper #72-958

6. "Sight Line Autopilot(SLAP) Phase 1 Final Report", D. R. Oelschlueger, A. J. VanDierendonck, T. G. Lahn. Honeywell Document 21729-FR, Nov 1971